Accounting for vapor liquid equilibrium in the modeling & simulation fof a commercial hydrotreating reactor

ARTICLE *in* INDUSTRIAL & ENGINEERING CHEMISTRY RESEARCH · DECEMBER 2010

Impact Factor: 2.59

1 AUTHOR:

Vinay P Mulgundmath

University of Ottawa

6 PUBLICATIONS **72** CITATIONS

SEE PROFILE

Accounting for Vapor−Liquid Equilibrium in the Modeling and Simulation of a Commercial Hydrotreating Reactor

Jinwen Chen,* Vinay Mulgundmath,[†] and Neil Wang[‡]

CanmetENERGY, Natural Resources Canada, One Oil Patch Drive, Devon, AB, Canada T9G 1A8

A one-dimensional, plug-flow, trickle-bed reactor model was developed to simulate a steady-state, adiabatic hydrotreating reactor with consideration of vapor−liquid equilibrium (VLE) effects. VLE calculations were simultaneously performed at each integration step of the model simulation. The thermophysical properties and mass flow rates of each fluid phase were updated as functions of local variables along the catalyst bed. Substantial differences in hydrodearomatization (HDA) and hydrodesulfurization (HDS) conversions were observed when the simulation was conducted with and without accounting for VLE, indicating the significance of VLE in the hydrotreater simulation. It was found that an increased inlet temperature increases HDS conversion but reduces HDA conversion. Increased pressure increases the reactor temperature and HDS and HDA conversions. Increased gas/oil ratio increases HDA conversion slightly, but does not change HDS conversion significantly. Polyaromatics are the most reactive for hydrogenation, and monoaromatics are the least reactive. Under the operating conditions investigated, both plug-flow and full catalyst wetting criteria are met, although significant vaporization of the liquid oil occurs in the commercial hydrotreating reactor.

1. Introduction

Middle-distillate hydrotreating (HDT) is one of the most important processes used in bitumen/heavy oil upgrading and petroleum refining to improve the quality of petroleum distillate fractions by removing sulfur, nitrogen, oxygen, and metals and by saturating olefins and aromatics. The HDT process is usually operated at temperatures of 300−400 °C and pressures of 30−100 bar in a fixed-bed catalytic reactor in the presence of hydrogen, with both the vapor and liquid phases flowing downward in trickle flow mode. Under such conditions, the process typically forms a vapor−liquid equilibrium (VLE) system, with both phases containing hydrogen and hydrocarbons due to the volatile nature of the oil and the high solubility of hydrogen in the oil.[1−5]

In a trickle-bed HDT reactor, hydrotreating reactions, including hydrodesulfurization (HDS), hydrodenitrogenation (HDN), and hydrodearomatization (HDA) occur on the catalyst surface (both external and internal), which is covered by liquid oil. There are complex couplings between the reactions, mass transfer, and heat transfer in this three-phase process. In traditional HDT reactor modeling and simulation, it is generally assumed that the feed oil is nonvolatile and that the flow rates of both the liquid and vapor phases therefore remain constant along the reactor. In fact, this assumption is not necessarily true for light- or middle-distillate HDT reactors. Our previous work, as well as some other published studies showed that relatively large amounts of hydrocarbons are present in the vapor phase, especially at higher temperatures, lower pressures, and/or higher gas/oil ratios.[1−7] Accordingly, it is necessary to take VLE into account to ensure accurate hydrotreater modeling and simulation. Moreover, commercial middle-distillate HDT reactors are operated under adiabatic conditions—temperature increases substantially along the catalyst bed, resulting in even more complex VLE behaviors and drastic changes in vapor and liquid phase flow rates, compositions, and thermophysical properties. Since the vaporization of oil requires a significant amount of heat, it is difficult to accurately predict reactor bed temperatures and performance if these changes are not accounted for.

Although efforts to model and simulate trickle-bed reactors have achieved considerable progress in combining transport phenomena and heterogeneous reactions,[8−15] variations in the flow rates and compositions of the individual phases due to the vaporization of liquid oil are often ignored because of the lack of VLE data and reliable prediction tools for HDT systems. Therefore, only a limited number of studies have been published investigating VLE effects in three-phase trickle-bed reactors, particularly in petroleum hydroprocessing reactors. Murali et al.[3] proposed a lumped two-phase plug-flow model to simulate both bench-scale and commercial diesel trickle-bed hydrotreaters. Under typical operating conditions significant feed vaporization (20−50%) was estimated and the model adequately predicted product quality, bed temperature profiles, and hydrogen consumption. Hoekstra[4] investigated VLE effects on ultra low sulfur diesel (ULSD) hydrotreating by varying the gas/oil ratio. The VLE effects were modeled by using the Frye-Mosby equation, which accounts for the effects of partial vaporization of feed and phase equilibrium on the reaction kinetics of individual sulfur compounds in trickle-bed hydrotreaters. Pellegrini et al.[5] developed a two-phase plug-flow reactor model to simulate the hydrocracking of Fischer−Tropsch synthesis products for diesel production. The simulation results showed that better agreement between experimental data and model prediction could be achieved by accounting for VLE. To quantify the partial liquid evaporation effect on HDS of dibenzothiophene in a trickle-bed hydrotreater, Kocis and Ho[16] treated the reactor as a series of smaller plug-flow reactors with interconnected vapor−liquid phase separators and concluded that neglecting the effect of solvent evaporation could results in

* To whom correspondence should be addressed. Tel.: 780 987 8763. Fax: 780 987 5349. E-mail: jichen@NRCan.gc.ca.

[†] Current address: Alberta Innovates-Technology Futures, 250 Karl Clark Road, Edmonton, AB, Canada T6N 1E4.

[‡] Current address: Kior Inc., 13001 Bay Park Road, Pasadena, TX 77507, United States.

10.1021/ie101550g
Published on Web 12/28/2010

misleading conclusions on reaction kinetics. Similar studies have been published by Avraam and Vasalos[17] who studied the VLE effects on hydrotreating reactor performance for light oil fractions, and by Bellos and Papayannakos[18] who investigated HDS kinetics using a three-phase microreactor. To our best knowledge no studies have been published to conduct simultaneous VLE calculation while the reactor model differential equations are being integrated along the reactor.

In our previous studies,[2,6,7] we conducted VLE flash experiments in a continuous-flow unit with hydrogen and various petroleum middle distillates under typical HDT conditions used in commercial operation. It was observed that the vaporization of oil greatly depends on the temperature, pressure, and gas/oil ratio, resulting in significant changes in the flow rates, chemical composition and thermophysical properties of both the vapor and liquid phases. A flash calculation program based on equations of state was specially developed to predict VLE in a hydrotreater under commercial operating conditions. In the VLE flash calculation, the oil feed is represented by 29 hydrocarbon pseudocomponents based on the simulated distillation (SimDis) data of the oil. The interaction coefficients between hydrogen and hydrocarbon pseudocomponents, which are required in the Peng−Robinson equation of state to perform VLE flash calculations, were estimated from experimental data and further correlated with the boiling points of the pseudocomponents and the aromatic content of the oil feed.[1,2] Using the VLE flash calculation program with the evaluated interaction coefficients, we demonstrated that, in pilot-plant trickle-bed hydrotreaters for petroleum middle distillates, VLE can significantly affect the flow hydrodynamics in the reactor.[1] It was concluded that process operating conditions and reactor configurations determine whether or not the pilot-plant hydrotreater operates under plug-flow and full catalyst wetting. Low temperature and gas/oil ratio, high pressure, small catalyst and/or diluting particle size, and a long catalyst bed all favor plug-flow and full catalyst wetting. It was also concluded that, under the same operating conditions and reactor configurations, the conditions for meeting the plug-flow criterion are more relaxed for light gas oil feed than for light cycle oil feed, even though both are middle distillates with similar boiling ranges.[1]

Continuing our investigation of VLE effects on trickle-bed reactors for middle-distillate hydrotreating, the present study explores the utilization of a steady-state trickle-bed reactor model coupled with simultaneous VLE calculation to predict commercial HDT reactor performance.

2. Reactor Model

To account for the vaporization of hydrocarbons, the mass transfer of each reacting component, including sulfur and aromatic compounds, to the gas phase must be included in the reactor model equations. Commercial HDT reactors usually have much larger ratios of bed diameter to particle diameter ($D_R/d_p > 1000 \gg 25$) than pilot-plant reactors, so the reactor wall effect is negligible, as suggested by Chu and Ng.[19] Considering the large ratio of catalyst bed length to particle size ($L_B/d_p > 1500$) and the high liquid velocities in commercial reactors, it is assumed that plug-flow and full catalyst wetting can be achieved. This will be verified during the reactor simulation as discussed later. On the basis of the above considerations, a one-dimensional plug-flow reactor (PFR) model that accounts for VLE is proposed with the following assumptions:

(1) Plug-flow and full catalyst wetting (to be verified during simulation).
(2) Adiabatic operation. No radial mass or heat transfer.
(3) No temperature gradient inside the catalyst and between the liquid and gas phases.
(4) VLE is achieved at the inlet and at any position inside the catalyst bed.
(5) Mass transfer in the gas phase is much faster than that in the liquid phase and faster than chemical reactions. No concentration difference between bulk gas and gas/liquid interface.
(6) All the sulfur compounds in the feed/product are treated as a single pseudosulfur component (total sulfur) with a single HDS reaction kinetics model.
(7) The aromatics and naphthenes in the feed and products are lumped into four groups: monoaromatics, diaromatics, polyaromatics (three or more aromatic rings), and naphthenes. Each group has its corresponding hydrogenation/dehydrogenation reaction kinetics.
(8) HDN is not considered in the reactor model.

The model consists of equations for mass and heat balances, VLE calculation, and boundary conditions as below:

Mass balance of species i in vapor phase

$$-\frac{d(u_G C_{G,i})}{dz} - k_{L,i} a_L (C^*_{L,i} - C_{L,i}) = 0 \quad (1)$$

Mass balance of species i in liquid phase

$$-\frac{d(u_L C_{i,L})}{dz} + k_{L,i} a_L (C^*_{L,i} - C_{L,i}) + R_i = 0 \quad (2)$$

u_G and u_L vary along the reactor axis due to hydrogen consumption, temperature change, and partial vaporization of oil. Calculations showed that u_G increases by about 10% while u_L decreases by about 20% from the inlet to the outlet of the reactor. The change in u_L occurs mostly at the very inlet of the reactor. To simplify the reactor model and the equation solving process, du_G/dz and du_L/dz are neglected while u_G and u_L are still calculated at each integration step to account for their changes. Equations 1 and 2 can then be simplified as

$$-u_G \frac{dC_{i,G}}{dz} - k_{L,i} a_L (C^*_{i,L} - C_{i,L}) = 0 \quad (1a)$$

$$-u_L \frac{dC_{i,L}}{dz} + k_{L,i} a_L (C^*_{i,L} - C_{i,L}) + \rho_b r_i = 0 \quad (2a)$$

Since HDT reactions are exothermic and commercial HDT reactors are normally operated in adiabatic mode, only one overall heat balance equation is required to account for the nonisothermal behavior in the reactor. It should be pointed out that since a significant amount of heat exchange occurs during oil vaporization and condensation, the enthalpy changes of the vapor and liquid phases are included in the present reactor model, as shown in eq 3 below, and are calculated through VLE using the Peng−Robinson equation of state:

$$-(\rho_G C_{p,G} u_G + \rho_L C_{p,L} u_L)\frac{dT}{dz} + (H_G - H_L)\frac{d\phi_G}{dT}\frac{dT}{dz} g_0 + \sum_j (-\Delta H^\circ_{r,j})\rho_b r_j = 0 \quad (3)$$

In eqs 1−3, species i represents H_2, H_2S, total sulfur, monoaromatics, diaromatics, polyaromatics, and naphthenes. The initial boundary conditions for the above ordinary differential equations (ODEs) are

$$z = 0: C_{i,G} = C_{i0,G},\ C_{i,L,} = C_{i0,L},\ T = T_0 \quad (4)$$

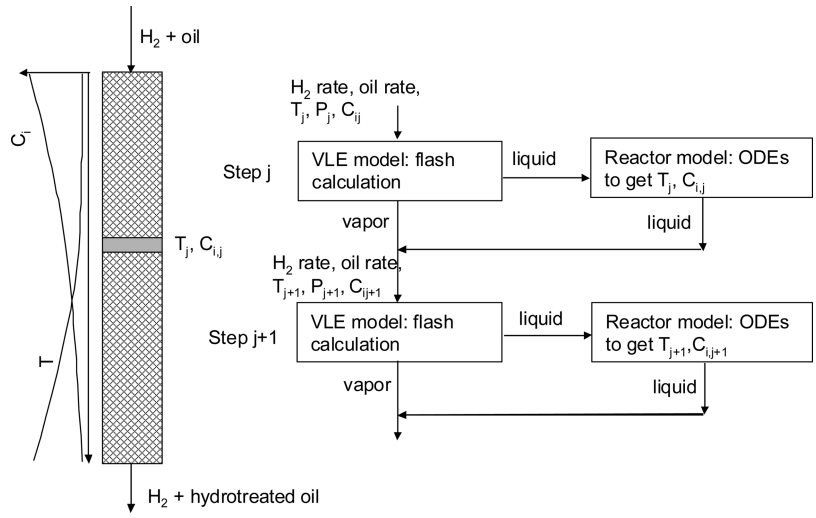

Figure 1. Schematic diagram of reactor modeling accounting for VLE.

VLE is achieved at the interface between the gas and liquid phases:

$$C_{i,\mathrm{L}}^{*} = \frac{C_{i,\mathrm{G}}}{K_i^{*}}\frac{C_{\mathrm{L}}}{C_{\mathrm{G}}} \tag{5}$$

The thermophysical properties, velocities, and flow rates of gas and liquid, as well as VLE, are functions of the temperature, pressure, and gas/oil ratio at any given axial position in the hydrotreating catalyst bed, which can be expressed in implicit form:

$$\left(\rho_{\mathrm{G}}, \rho_{\mathrm{L}}, C_{p,\mathrm{G}}, C_{p,\mathrm{L}}, \mu_{\mathrm{G}}, \mu_{\mathrm{L}}, u_{\mathrm{G}}, u_{\mathrm{L}}, H_{\mathrm{G}}, H_{\mathrm{L}}, \frac{\mathrm{d}\phi_{\mathrm{G}}}{\mathrm{d}T}, K_i^{*}\right) = f(T, P, \mathrm{G/O}) \tag{6}$$

Equations 1a, 2a, and 3 are first-order ODEs with initial boundary conditions (eq 4), which are solved numerically using the Runge−Kutta method.[20] Equation 5 represents VLE that is calculated simultaneously by using the flash program when eqs 1a, 2a, and 3 are integrated. Equation 6 gives the thermophysical properties of the vapor and liquid phases as implicit functions of reactor temperature, pressure, and gas/oil ratio at any axial position in the catalyst bed. These properties are estimated in the VLE flash program by means of various correlations. A schematic diagram of the reactor model coupled with VLE calculation is shown in Figure 1.

3. Reaction Kinetics and Model Parameters

In an HDT process for petroleum middle distillates, there are many different types of reactions that are very complex and not fully understood in spite of considerable research effort. Appropriate simplifications are necessary when considering these reactions, which involve hundreds or even thousands of sulfur, nitrogen, and aromatic compounds. Among the HDT reactions, HDS and HDA reactions contribute the most to the total heat of reactions;[21,22] therefore, only HDS and HDA are considered in the present model. The total heat of reactions plays a critical role in reactor simulation. However scattered values of this important parameter have been reported in the literature ranging from 50−80 kJ/mol hydrogen for different reactions. In this work, the values of 60 and 67 kJ/mol hydrogen for HDS and HDA reactions, respectively, are used, which were recommended by Chowdhury et al.[14] The simplified reaction schemes are represented by the following reactions:

Table 1. Kinetic Parameters and Heats of Reaction

reaction	parameter values
HDS	$\nu_{\mathrm{HDS}} = 3$, $n_1 = 1.6$, $n_2 = 0.56$ $k_{\mathrm{HDS}} = 2.5 \times 10^9 \exp(-19384.0/T)$, $K_{\mathrm{H_2S}} = 5 \times 10^4$, $-\Delta H^{\circ}_{\mathrm{r,HDS}} = -60.3 \times 10^3$ J/mol H_2
HAD	$\nu_{\mathrm{HDA1}} = 2$, $\nu_{\mathrm{HDA2}} = 2$, $\nu_{\mathrm{HDA3}} = 3$, $n_{\mathrm{HDA1}} = 0.5$, $n_{\mathrm{HDA2}} = 0.5$, $n_{\mathrm{HDA3}} = 1.0$ $k_{\mathrm{HDA1}} = 2.66 \times 10^5 \exp(-15170/T)$, $k_{\mathrm{HDA2}} = 8.50 \times 10^2 \exp(-12140/T)$, $k_{\mathrm{HDA3}} = 6.04 \times 10^2 \exp(-12414/T)$ $K_{\mathrm{HDA1}} = 1.5073 \times 10^{-5} \exp(-8308/T)$, $K_{\mathrm{HDA2}} = 5.566 \times 10^{-11} \exp(-15740/T)$, $K_{\mathrm{HDA3}} = 7.4928 \times 10^{-17} \exp(-24070/T)$ $-\Delta H^{\circ}_{\mathrm{r,HDA}} = -67.0 \times 10^3$ J/mol H_2

HDS reaction

$$\mathrm{AS} + \nu_{\mathrm{HDS}}\mathrm{H_2} \rightarrow \mathrm{A} + \mathrm{H_2S} \tag{7}$$

where AS and A represent total organic sulfur and the resulting hydrocarbons, respectively.

HDA reactions

$$\mathrm{PA} + \nu_{\mathrm{HDA1}}\mathrm{H_2} \leftrightarrow \mathrm{DA} \tag{8}$$

$$\mathrm{DA} + \nu_{\mathrm{HDA2}}\mathrm{H_2} \leftrightarrow \mathrm{MA} \tag{9}$$

$$\mathrm{MA} + \nu_{\mathrm{HDA3}}\mathrm{H_2} \leftrightarrow \mathrm{NA} \tag{10}$$

where MA, DA, PA, and NA represent monoaromatics, diaromatics, polyaromatics, and naphthenes, respectively.

The kinetic models and their corresponding parameters for each of the above reactions are different from different sources due to the differences in the catalysts, properties of the feeds, reaction conditions, and experimental methods used in obtaining the kinetics. In this paper, the kinetic models were taken from the literature[14,15] and are represented by eqs 11 and 12. The relevant kinetics model parameters are summarized in Table 1.

HDS kinetics

$$-r_{\mathrm{HDS}} = \frac{k_{\mathrm{HDS}} C_{\mathrm{s}}^{n_1} C_{\mathrm{H_2}}^{n_2}}{(1 + K_{\mathrm{H_2S}} C_{\mathrm{H_2S}})^2} \tag{11}$$

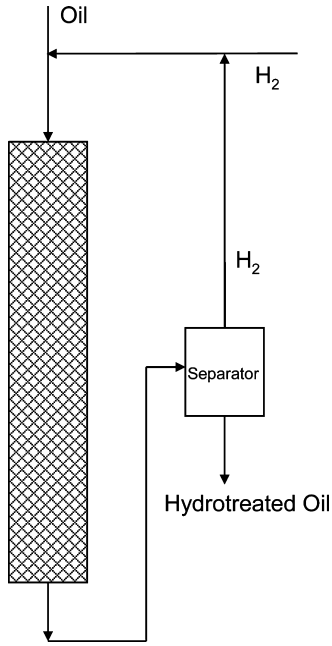

Figure 2. Schematic diagram of a single-stage middle-distillate hydrotreater.

HDA kinetics

$$-r_{\mathrm{HDA1}} = -k_{\mathrm{HDA1}} P_{H_2}^{n_{\mathrm{HDA1}}} (C_{\mathrm{PA}} - C_{\mathrm{DA}}/K_{\mathrm{HDA1}})$$

$$-r_{\mathrm{HDA2}} = -k_{\mathrm{HDA2}} P_{H_2}^{n_{\mathrm{HDA2}}} (C_{\mathrm{PA}} - C_{\mathrm{DA}}/K_{\mathrm{HDA2}})$$

$$-r_{\mathrm{HDA3}} = -k_{\mathrm{HDA3}} P_{H_2}^{n_{\mathrm{HDA3}}} (C_{\mathrm{PA}} - C_{\mathrm{DA}}/K_{\mathrm{HDA3}}) \quad (12)$$

Other parameters required in the reactor model equations were calculated using literature correlations:[23]

$$\frac{K_{\mathrm{L},i} a_{\mathrm{L}}}{D_{i,\mathrm{L}}} = 7\left(\frac{\rho_{\mathrm{L}} \mu_{\mathrm{L}}}{\mu_{\mathrm{L}}}\right)^{0.4}\left(\frac{\mu_{\mathrm{L}}}{\rho_{\mathrm{L}} D_{i,\mathrm{L}}}\right)^{0.5} \quad (13)$$

$$D_{i,\mathrm{L}} = 8.93 \times 10^{-8}\left(\frac{v_{\mathrm{L}}^{0.267}}{v_i^{0.433}}\right)\left(\frac{T}{\mu_{\mathrm{L}}}\right) \quad (14)$$

4. Reactor Configuration and Operating Conditions

To simplify the simulation, a single-stage adiabatic commercial HDT reactor without interstage quenching was employed. The reactor configuration and the operating conditions used for the simulation are as follows:

Catalyst bed length: 9 m
Catalyst bed diameter: 3.5 m
Feed: light gas oil (LGO)
Liquid hourly space velocity (LHSV): 1.5/h
Gas/oil ratio: 600, 700, 800, 900 NL/kg
Temperature: 340, 350, 360, 370, 380 °C
Pressure: 40, 50, 60, 70 bar

A schematic diagram of the single-stage hydrotreater is shown in Figure 2.

The properties of the middle-distillate feedstock LGO are listed in Table 2. It is commercial straight-run light gas oil containing 26.8 wt % aromatics and 1.216 wt % total sulfur.

5. Results and Discussion

5.1. VLE Modeling and Validation. As mentioned in the introduction section, the VLE calculation program used in this study was specially developed for petroleum hydroprocessing systems. Flash experiments were conducted to obtain VLE data with different types of middle distillates, and at different temperatures and pressures. The VLE data were then used to estimate the interaction coefficients between hydrogen and hydrocarbon pseudocomponents, which were further correlated with the boiling points of the pseudocomponents and the aromatic content of the oil feed. The details can be found in our previously published papers.[1,2]

Table 2. Properties of the Feedstock

	LGO
density (15.6 °C), g/cm^3 (ASTM D4052)	0.8392
saturates, wt %	73.2
paraffins	64.2
naphthenes	9.0
aromatics, wt %	26.8
monoaromatics	12.1
diaromatics	9.3
polyaromatics	5.4
sulfur, wt %	1.216
SimDis, °C (ASTM D2887)	
IBP	126.5
10 wt %	214.5
30 wt %	262.5
50 wt %	295.0
70 wt %	326.5
90 wt %	370.5
FBP	435.0

$$d_{i\mathrm{H}} = A + B \times \mathrm{BP}_i \quad (15)$$

$$A = 0.3852 - 0.00241 \times C_{\mathrm{Aromatics\%}} \quad (16)$$

$$B = 0.002245 + 1.96 \times 10^{-5} \times C_{\mathrm{Aromatics\%}} \quad (17)$$

Equations 15−17 were developed with experimental data obtained in the temperature range of 250−400 °C, pressure range of 50−100 bar, and with three different types of middle distillates. It is expected that these correlations can be used with any type of middle distillates as long as the total aromatics content in the oil feed is known.

The interaction coefficients between hydrogen and hydrocarbon pseudocomponents play an important role in VLE calculation. They cannot be ignored or simply set to zero since the VLE calculation results are sensitive to the change in their values. Figure 3 illustrates the comparison of VLE calculation results with the interaction coefficients calculated from eqs 15−17 and with the interaction coefficients set to zero for a hydrogen−light cycle oil system which has been previously

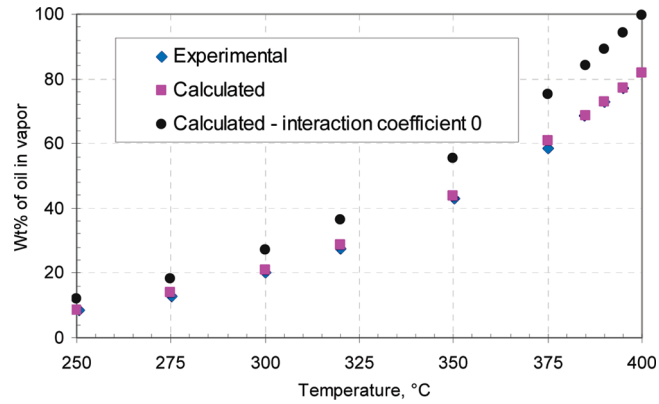

Figure 3. Comparison of VLE calculation results with and without interaction coefficients.

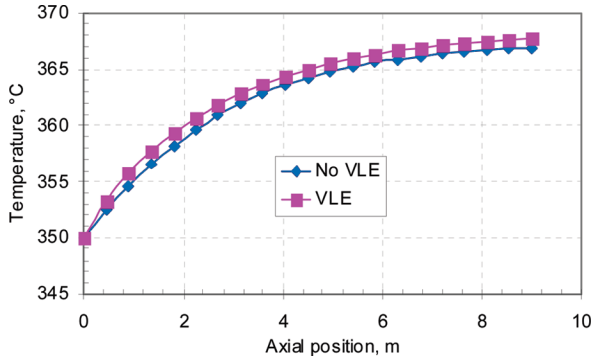

Figure 4. Axial temperature profiles with and without VLE (T_0 = 350 °C, P = 50 bar, LHSV = 1.5/h, gas/oil ratio = 800 NL/kg).

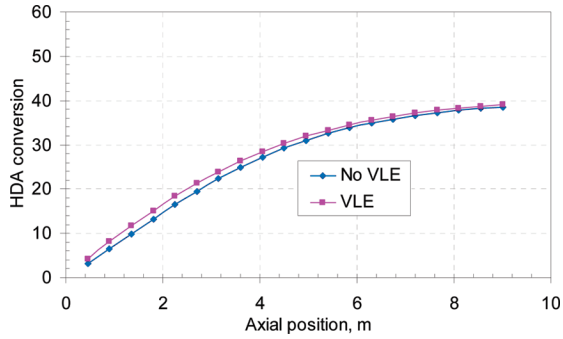

Figure 5. HDA conversion with and without VLE (T_0 = 350 °C, P = 50 bar, LHSV = 1.5/h, gas/oil ratio = 800 NL/kg).

reported.[1,2] It is clear in Figure 3 that the VLE calculation results (weight percent of oil vaporized into the vapor phase) with the calculated interaction coefficients from eqs 15−17 are quite close to those measured from experiment while the ones with the interaction coefficients set to zero are much higher than those measured experimentally. Therefore accurate estimation of the interaction coefficients between hydrogen and hydrocarbon pseudocomponents is critical to the VLE modeling and calculation of petroleum hydroprocessing systems.

5.2. Comparison of Simulation Results With and Without Accounting for VLE. To demonstrate VLE effects, hydrotreater simulations were conducted using the same reactor model, kinetics, and other parameters, as discussed above, with and without accounting for VLE in the reactor model. In the simulation without accounting for VLE, it was simply assumed that all the LGO feed was in the liquid phase in the reactor. Figure 4 shows the axial temperature profiles in the catalyst bed predicted with and without accounting for VLE; they are typical adiabatic operating temperature profiles for exothermic reactions. As seen in the figure, the model with VLE predicted temperatures of about 1 °C higher than the one without VLE. Some differences are also observed for HDA and HDS conversions as shown in Figures 5 and 6, respectively.

It is assumed that VLE is achieved at the reactor inlet under the inlet temperatures and pressures. Therefore only the vaporization that was caused by the temperature rise in the reactor required additional heat. The reactor temperature depended on two factors: the total HDS conversion and the total amount of aromatics that were converted through the three hydrogenation reactions. As seen in Figure 5, the total HDA conversion with VLE was slightly higher than that without VLE while the total HDS conversion with VLE was much higher than that without VLE as seen in Figure 6. Therefore more heat was released in the case with VLE. This extra amount of heat

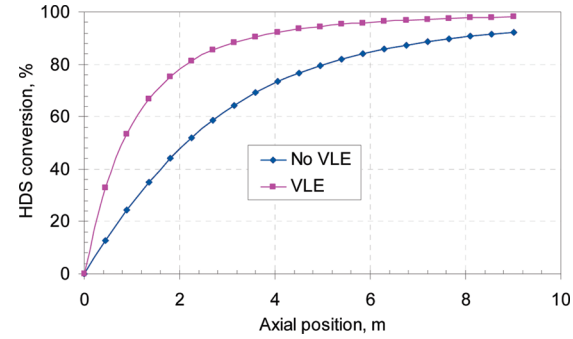

Figure 6. HDS conversion with and without VLE (T_0 = 350 °C, P = 50 bar, LHSV = 1.5/h, gas/oil ratio = 800 NL/kg).

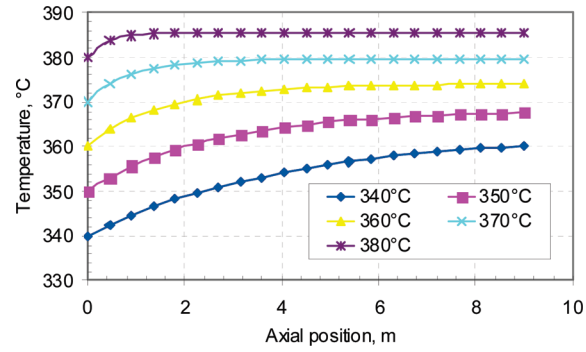

Figure 7. Axial temperature profiles at different inlet temperatures with VLE (P = 50 bar, LHSV = 1.5/h, gas/oil ratio = 800 NL/kg).

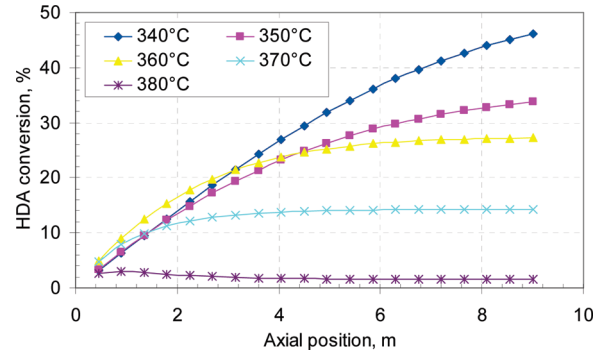

Figure 8. HDA conversion at different inlet temperatures with VLE (P = 50 bar, LHSV = 1.5/h, gas/oil ratio = 800 NL/kg).

was used to partially vaporize the oil inside the reactor and to heat the reactor by 1 °C higher than that without VLE as shown in Figure 4.

5.3. Effects of Inlet Temperature. While accounting for VLE effects in the reactor model, simulations were performed at different inlet temperatures (T_0), namely 340, 350, 360, 370, and 380 °C, while the other operating conditions were fixed: P = 50 bar, LHSV = 1.5/h, gas/oil ratio = 800 NL/kg. Figures 7−10 show the simulation results. Figure 7 shows the axial temperature profiles in the catalyst bed at different inlet temperatures. As seen in the figure, at the lowest T_0 of 340 °C, the axial temperature gradient is the steepest, with a rise of about 20 °C from inlet to outlet, indicating that significant heat is released from the hydrotreating (mainly HDA) reactions. Therefore, the overall HDA conversion should be the highest in this case, which is confirmed by the HDA conversion plots in Figure 8. The temperature gradients become flatter as T_0 increases. At the highest T_0 of 380 °C, the temperature increases by only about 6 °C from the inlet to the outlet of the reactor,

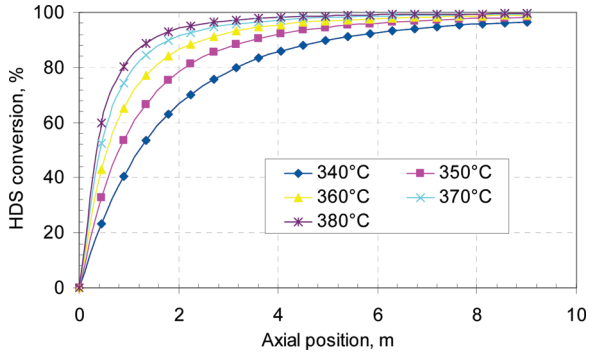

Figure 9. HDS conversion at different inlet temperatures with VLE (P = 50 bar, LHSV = 1.5/h, gas/oil ratio = 800 NL/kg).

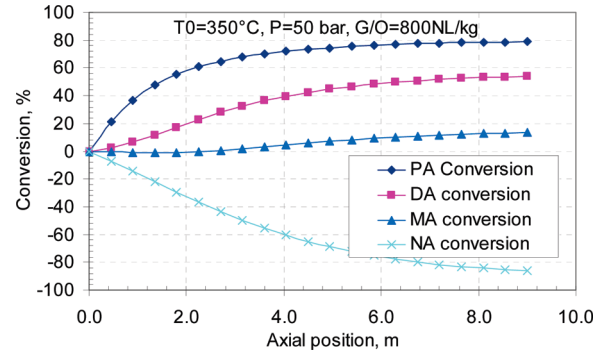

Figure 10. Individual hydrocarbon lump conversion with VLE (T_0 = 350 °C, P = 50 bar, LHSV = 1.5/h, gas/oil ratio = 800 NL/kg).

indicating very little heat release and low HDA conversion, as seen in Figure 8.

Figure 8 also shows that, at the lowest T_0 of 340 °C, the HDA conversion is the highest at about 44%, while at the highest T_0 of 380 °C, the HDA conversion is the lowest at only about 2%. In this latter case, the temperature actually remains almost constant along the catalyst bed. These observed trends are attributed to the reversible nature of the HDA reactions (hydrogenation/dehydrogenation). Since all the HDA reactions are exothermic and reversible, high temperature favors the reverse (dehydrogenation) reactions. As seen in Figure 7, at the highest T_0 of 380 °C, the temperature in the catalyst bed is among the highest (although the temperature gradient is the flattest), at about 386 °C. At this temperature, the dehydrogenation reactions outpace the hydrogenation reactions, resulting in reduced HDA conversion, as seen in Figure 8. Cheng et al.[24] also reported that 380 °C is the upper temperature limit that can be practically employed in hydrotreating diesel fuel in order to prevent the domination of dehydrogenation reactions. It was observed that the temperature at which the dehydrogenation reactions become dominant depends on other operating conditions, such as pressure and LHSV, although VLE or liquid feed vaporization may also play an important role in the observed trends as reported by Wilson and Kriz.[25] Figure 9 shows the HDS conversions at different T_0 values. In contrast to the trend observed with HDA conversion, HDS conversion always increases with increasing T_0 as seen in the figure. HDS conversion exhibits a sharp increase in the first 2 m of the catalyst bed and then tends to level off toward the outlet of the reactor. This trend becomes more evident as T_0 increases. At the highest T_0 of 380 °C, the HDS conversion does not change much beyond the axial position of about 4 m, meaning that the rest of the catalyst bed is not being efficiently utilized in terms of HDS conversion.

Figure 10 shows the conversions of individual hydrocarbon lumps along the catalyst bed at T_0 = 350 °C, while other operating conditions are the same as those in Figures 7−9. As illustrated in Figure 10, the conversions of PA, DA, and MA increase along the catalyst bed from inlet to outlet. The conversion of NA decreases along the catalyst bed, with negative values, meaning that naphthenes are formed (instead of converted) from the hydrogenation of aromatics and that their amounts increase along the catalyst bed. It is also noted that, of the three aromatic lumps, PA has the highest conversion while MA has the lowest, with DA in between. Accordingly, PA is the most reactive for hydrogenation and MA is the least reactive. Similar observations have also been reported by other researchers.[14,22,24,26,27]

5.4. Effects of Gas/Oil Ratio. Simulations were conducted at gas/oil ratios of 600, 700, 800, and 900 NL/kg while other

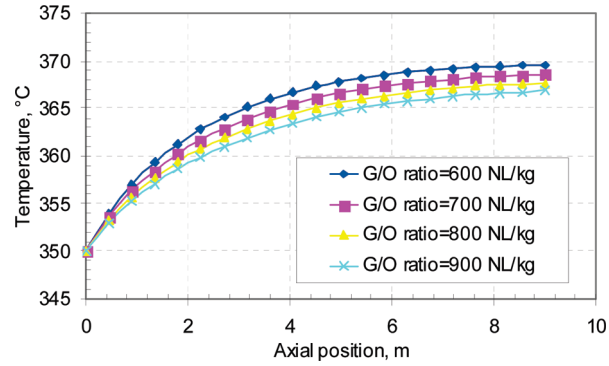

Figure 11. Reactor temperature profiles at different gas/oil ratios with VLE (T_0 = 350 °C, P = 50 bar, LHSV = 1.5/h).

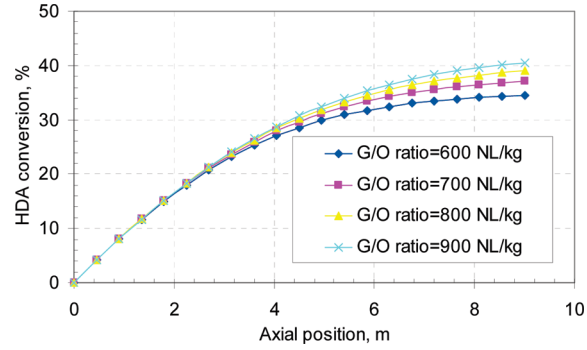

Figure 12. HDA conversion at different gas/oil ratios with VLE (T_0 = 350 °C, P = 50 bar, LHSV = 1.5/h).

conditions were fixed at T_0 = 350 °C, P = 50 bar, and LHSV = 1.5/h. The simulation results are shown in Figures 11−13. As seen in Figure 11, with increasing gas/oil ratio, the reactor temperature decreases slightly. This is understandable and attributed to (1) increased vaporization of liquid oil as the gas flow increases and (2) increased hydrogen flow that absorbs more heat. The HDA conversion also increases slightly with increasing gas/oil ratio as observed in Figure 12, which results from increased reaction rates (eq 12) due to increased hydrogen partial pressure in the vapor phase. The slightly reduced reactor temperature might also have contributed to the increased HDA conversion as discussed above. It seems that increasing the gas/oil ratios does not have a significant impact on HDS conversion compared to the effect on HDA conversion, as shown in Figure 13. At all the gas/oil ratios used, the HDS conversions approach 100 at the outlet of the catalyst bed.

5.5. Effects of Pressure. Hydrotreater simulations were conducted at different pressures (40, 50, 60, 70 bar), while other operating conditions were fixed at T_0 = 350 °C, LHSV = 1.5/

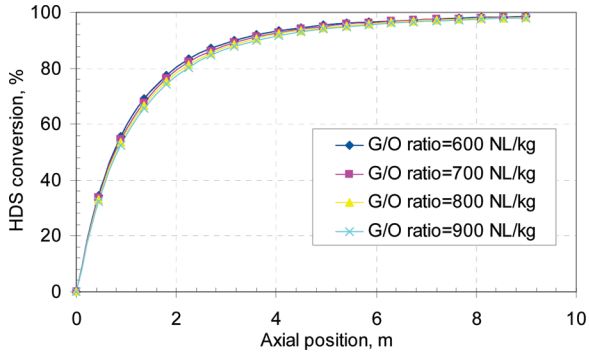

Figure 13. HDS conversion at different gas/oil ratios with VLE (T_0 = 350 °C, P = 50 bar, LHSV = 1.5/h).

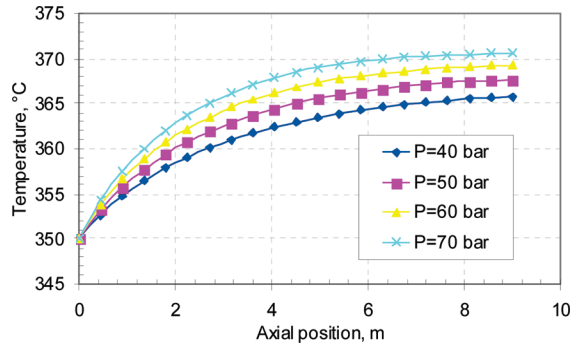

Figure 14. Reactor temperature profiles at different pressures with VLE (T_0 = 350 °C, LHSV = 1.5/h, gas/oil ratio = 800 NL/kg).

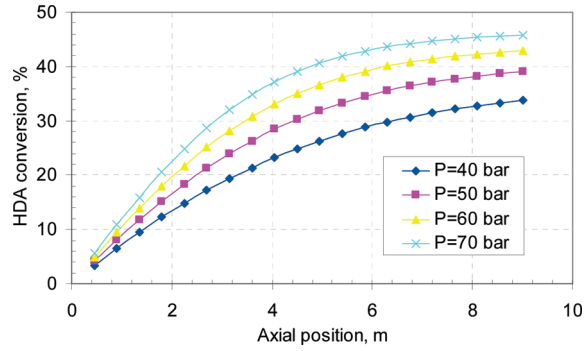

Figure 15. HDA conversion at different pressures with VLE (T_0 = 350 °C, LHSV = 1.5/h, gas/oil ratio = 800 NL/kg).

h, and gas/oil ratio = 800 NL/kg. The simulation results are shown in Figures 14−16. As seen in Figure 14, increasing the pressure resulted in increased reactor temperature. There are two factors that caused the increase: increased hydrogen partial pressure that leads to increased HDS and HDA reaction rates and reduced vaporization of liquid oil. Increased pressure also has a significantly positive effect on HDA conversion as shown in Figure 15. The total HDA conversion increased from 32% at 40 bar to 44% at 70 bar. From a kinetics point of view, increasing the pressure results in increased hydrogen partial pressure to increase the reaction rate (eq 12). From a thermodynamics point of view, increased pressure moves the hydrogenation/dehydrogenation chemical equilibrium in the hydrogenation direction, resulting in increased HDA conversion. The effect of increasing pressure on HDS conversion is substantial only in the first half of the catalyst bed, as seen in Figure 16. Near the outlet of the catalyst bed, the HDS conversion

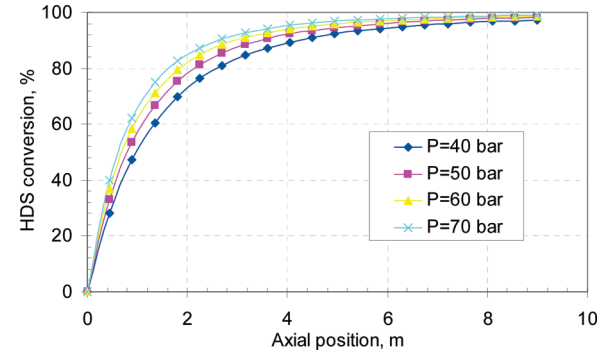

Figure 16. HDS conversion at different pressures with VLE (T_0 = 350 °C, LHSV = 1.5/h, gas/oil ratio = 800 NL/kg).

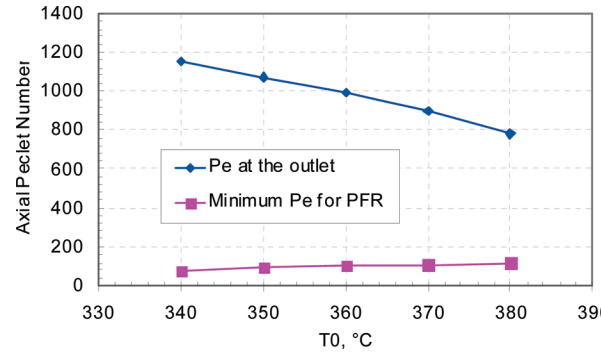

Figure 17. Plug-flow verification at different inlet temperatures (P = 50 bar, LHSV = 1.5/h, gas/oil ratio = 800 NL/kg).

approaches 100% and only minor differences are observed for the HDS conversions at different pressures.

5.6. Verification of Plug-Flow and Full Catalyst Wetting. As mentioned earlier, the reactor model assumes plug-flow and full catalyst wetting. Calculations were performed to verify these assumptions. The criteria and the calculation procedure can be found in our previously published paper.[1] As discussed above, the temperature increases along the catalyst bed, resulting in increased vaporization of oil and reduced liquid phase flow rate. Under any given operating conditions, the outlet of the catalyst bed is where the liquid flow rate is the lowest and the plug-flow and full catalyst wetting criteria are the most difficult to meet. Therefore, the calculations were performed at the outlet of the catalyst bed. Figure 17 shows the actual Peclet number (Pe) of the liquid phase and the minimum Peclet number required to meet the plug-flow criterion at different inlet temperatures (other conditions are the same as those used in Figures 7−9). It is seen that, at all the inlet temperatures, the actual Pe values at the catalyst bed outlet are much higher than the minimum values required to meet the plug-flow criterion, meaning that the plug-flow assumption is valid. Figure 18 shows the actual catalyst wetting number at the outlet of the catalyst bed and the minimum wetting number required to maintain full catalyst wetting. The actual wetting number is higher than the minimum at all inlet temperatures. However, as the inlet temperature increases, the two approach each other. At an inlet temperature of 380 °C, they are almost the same, meaning that any further increase in inlet temperature would result in incomplete catalyst wetting. Calculations performed at other conditions investigated in this study show that both plug-flow and full catalyst wetting criteria are met. The results will not be shown here. Therefore, in a commercial hydrotreater, incomplete catalyst wetting is more of a concern than plug-

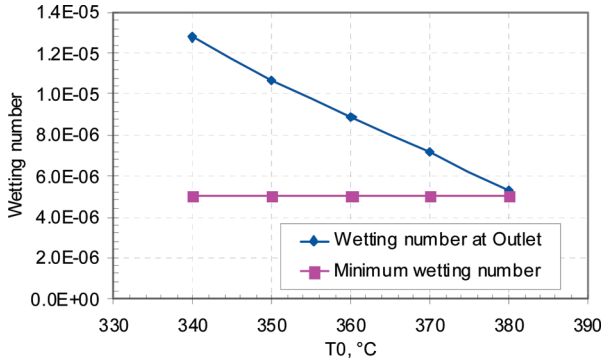

Figure 18. Full catalyst wetting verification at different inlet temperatures (P = 50 bar, LHSV = 1.5/h, gas/oil ratio = 800 NL/kg).

flow if the reactor temperature is high, the pressure is low, and/or the gas/oil ratio is high.

6. Conclusions

In this paper, VLE effects were considered in the simulation of commercial-scale middle-distillate hydrotreaters using a one-dimensional plug-flow reactor model. VLE calculations were performed using a calibrated flash program based on equations of state. It was concluded that

(1) Substantial differences in hydrodearomatization and hydrodesulfurization conversions were observed when the simulation was conducted with and without accounting for VLE, while noticeable differences were observed in the axial temperature profiles, indicating the significance of VLE in the hydrotreater simulation.

(2) Increased inlet temperature increases HDS conversion but reduces HDA conversion. Increased pressure increases reactor temperature, and HDS and HDA conversions. Increased gas/oil ratio increases HDA conversion slightly, but does not change HDS conversion significantly.

(3) Polyaromatics, diaromatics, and monoaromatics have net positive conversions, resulting in net naphthenes generation. Polyaromatics are the most reactive for hydrogenation, and monoaromatics are the least reactive. At a reactor temperature of about 386 °C, the dehydrogenation reactions outpace the hydrogenation reactions and become dominant, resulting in increased aromatics content in the hydrotreated product.

(4) Under the operating conditions investigated, both plug-flow and full catalyst wetting criteria are met, although significant vaporization of the liquid oil occurs in the commercial hydrotreating reactor.

Accurate modeling and simulation of middle-distillates/diesel hydrotreating reactors to predict product composition and quality is of importance and interest to both commercial operation and research and development (RD). Accounting for VLE in trickle-bed reactor modeling has great potential to improve the capability and predictability of the models, and therefore, more research effort should be made on this subject. Further modeling and simulation work should be done with actual commercial hydrotreater configuration (multistage with interstage quenching). The simulation results should be compared with commercial data to demonstrate the necessity and advantage for accounting for VLE and to validate the model predicting capability.

Acknowledgment

Partial funding for this study was provided by the Canadian interdepartmental Program of Energy Research and Development (PERD).

Nomenclature

A = correlation parameter defined in eq 15
a_L = liquid effective surface area, m^2/m^3
B = correlation parameter defined in eq 15, 1/°C
C = concentration, $kmol/m^3$
C_p = heat capacity, kJ/(kg·K)
$C_{Aromatics\%}$ = aromatics content in oil feed, wt %
D_L = liquid diffusion coefficient, cm^2/s
D_R = diameter of reactor bed, cm
d_{iH} = interaction coefficient between hydrogen and hydrocarbon pseudocomponents
g = acceleration due to gravity (9.81 m/s^2)
H = enthalpy, kJ/kmol
ΔH_r^0 = heat of reaction, kJ/mol
K_{HDA1} = hydrogenation equilibrium constant (polyaromatics), dimensionless
K_{HDA2} = hydrogenation equilibrium constant (diaromatics), dimensionless
K_{HDA3} = hydrogenation equilibrium constant (monoaromatics), dimensionless
K_{H_2S} = adsorption equilibrium constant of H_2S, $m^3/kmol$
K^* = VLE constant, dimensionless
k_L = liquid mass transfer coefficient, m/s
k_{HDS} = HDS reaction rate constant, $(m^3)^{2.16}/(kg \cdot kmol^{1.16} \cdot s)$
k_{HDA1} = hydrogenation reaction rate constant (polyaromatics), $m^3/(kg \cdot s)$
k_{HDA2} = hydrogenation reaction rate constant (diaromatics), $m^3/(kg \cdot s)$
k_{HDA3} = hydrogenation reaction rate constant (monoaromatics), $m^3/(kg \cdot s)$
L_B = reactor bed length, cm (or m)
n = reaction order
P = pressure, atm or MPa
Pe = Peclet number
r = reaction rate, kmol/(kg·s)
T = temperature, °C or K
u = superficial velocity, m/s
z = reactor axial position, m

Subscripts

b = catalyst bed
DA = diaromatics
G = gas phase
H_2 = hydrogen
H_2S = hydrogen sulfide
i = component i
j = reaction j
L = liquid phase
MA = monoaromatics
NA = naphthenes
PA = polyaromatics
S = sulfur
0 = inlet

Superscripts

* = VLE

Greek Symbols

μ = viscosity (cP)
ρ = liquid phase density, g/cm^3

Φ = vaporization fraction
ν = stoichiometric coefficient

Abbreviations

AS = organic sulfur
DA = diaromatics
G/O = gas/oil ratio
HDA = hydrodearomatization
HDN = hydrodenitrogenation
HDS = hydrodesulfurization
ID = internal diameter, cm
LCO = light cycle oil
LGO = light gas oil
LHSV = liquid hourly space velocity
MA = monoaromatics
NA = naphthenes
ODE = ordinary differential equation
PA = polyaromatics
PDE = partial differential equation
PFR = plug-flow reactor
VLE = vapor−liquid equilibrium

Literature Cited

(1) Chen, J.; Wang, N.; Fabián, S. M.; Jorge, A. Vapor-Liquid Equilibrium Study in Trickle Bed Reactors. *Ind. Eng. Chem. Res.* **2009**, *48*, 1096–1106.

(2) Chen, J.; Jiang, W.; Yang, H.; Hawkins, R.; Ring, Z. Comparative Study of Vapor-Liquid Equilibrium during Hydroporcessing of Different Petroleum Feedstocks. *Proceedings of the 2006 AIChE National Spring Meeting*, Orlando, FL, April 23−27, 2006.

(3) Murali, C.; Voolapalli, R. K.; Ravichander, N.; Gokak, D. T.; Choudary, N. V. Trickle Bed Reactor Model to Simulate the Performance of Commercial Diesel Hydrotreating Unit. *Fuel* **2007**, *86*, 1176–1184.

(4) Hoekstra, G. The Effect of Gas-to-Oil rate in Ultra Low Sulphur Diesel Hydrotreating. *Catal. Today* **2007**, *127*, 99–102.

(5) Pellegrini, L. A.; Gamba, S.; Calemma, V.; Bonomi, S. Modeling of Hydrocracking with Vapor-Liquid Equilibrium. *Chem. Eng. Sci.* **2008**, *63*, 4285–4291.

(6) Chen, J.; Ring, Z. Vapor-Liquid Phase Equilibrium during Hydrotreating of Light Cycle Oil. *Proceedings of the 2004 AIChE National Spring Meeting*, New Orleans, LA, April 25−29, 2004.

(7) Chen, J.; Yang, H.; Ring, Z. Experimental Study on Vapor-Liquid Phase Equilibrium of LCO Hydrotreating Systems at High Temperatures and Pressures. *Proceedings of the 2005 AIChE National Spring Meeting*, Atlanta, GA, April 10−14, 2005.

(8) Garcia, C. L.; Hudebine, D.; Schweitzer, J. M.; Ferre, V. D. In-depth Modeling of Gas Oil Hydrotreating: From Feedstock Reconstruction to Reactor Stability Analysis. *Catal. Today* **2010**, *150*, 279–299.

(9) Alvarez, A.; Ancheyta, J.; Munoz, J. A. D. Modeling, Simulation and Analysis of Heavy Oil Hydroprocessing in Fixed-Bed Reactors Employing Liquid Quench Streams. *Appl. Catal. A: Gen.* **2009**, *361*, 1–12.

(10) Gunjal, P. R.; Ranade, V. V. Modeling of Laboratory and Commercial Scale Hydro-Processing Reactors Using CFD. *Chem. Eng. Sci.* **2007**, *62*, 5512–5526.

(11) Mederos, F. S.; Rodriguez, M. A.; Ancheyta, J.; Arce, E. Dynamic Modeling and Simulation of Catalytic Hydrotreating Reactors. *Energy Fuels* **2006**, *20*, 936–945.

(12) Bellos, G. D.; Kallinikos, L. E.; Gounaris, C. E.; Papayannakos, N. G. Modeling of the Performance of Industrial HDS Reactors Using a Hybrid Neural Network Approach. *Chem. Eng. Proc.* **2005**, *44*, 505–515.

(13) Bhaskar, M.; Valavarasu, G.; Sairam, B.; Balaraman, K. S.; Balu, K. Three-Phase Reactor Model to Simulate the Performance of Pilot-Plant and Industrial Trickle-Bed Reactors Sustaining Hydrotreating Reactions. *Ind. Eng. Chem. Res.* **2004**, *43*, 6654–6669.

(14) Chowdhury, R.; Pedernera, E.; Reimert, R. Trickle-Bed Reactor Model for Desulfurization and Dearomatization Diesel. *AIChE J.* **2002**, *48*, 126–135.

(15) Korsten, H.; Hoffmann, U. Three-Phase Reactor Model for Hydrotreating in Pilot Plant Trickle-Bed Reactors. *AIChE J.* **1996**, *42*, 1350–1360.

(16) Kocis, G. R.; Ho, T. C. Effects of Liquid Evaporation on the Performance of Trickle-Bed Reactors. *Chem. Eng. Res. Des.* **1986**, *64*, 288–291.

(17) Avraam, D. G.; Vasalos, I. A. HdPro: A Mathematical Model of Trickle-bed Reactors for the Catalytic Hydroprocessing of Oil Feedstocks. *Catal. Today* **2003**, *79−80*, 275–283.

(18) Bellos, G. D.; Papayannakos, N. G. The Use of a Three Phase Microreactor to Investigate HDS Kinetics. *Catal. Today* **2003**, *79&80*, 349–355.

(19) Chu, C. F.; Ng, K. M. Flow in Packed Tubes with a Small Tube to Particle Diameter Ratio. *AIChE J.* **1989**, *35*, 148–158.

(20) Hindmarsh, A. C. *ODEPACK, A Systematized Collection of ODE Solvers in Scientific Computing*; Stepleman, R. S., et al.; Eds.; North-Holland: Amsterdam, 1983.

(21) Jaffe, S. B. Kinetics of heat release in petroleum hydrogenation. *Ind. Eng. Chem. Proc. Res. Dev.* **1974**, *13*, 34–39.

(22) Stanislaus, A.; Cooper, B. H. Aromatic hydrogenation catalysis: A Review. *Catal. Rev. Sci. Eng.* **1994**, *36*, 75–123.

(23) Goto, S.; Smith, J. M. Trickle-bed Reactor Performance. Part I. Holdup and Mass Transfer Effects. *AIChE J.* **1975**, *21*, 706–713.

(24) Cheng, Z. M.; Fang, X. C.; Zeng, R. H.; Han, B. P.; Huang, L.; Yuan, W. K. Deep Removal if Sulphur and Aromatics from Diesel through Two-stage Cocurrently and Countercurrently Operated Fixed Bed Reactors. *Chem. Eng. Sci.* **2004**, *59*, 5465–5472.

(25) Wilson, M. F.; Kriz, J. F. Upgrading of Middle Distillate Fractions of a Syncrude from Athabasca Oil Sands. *Fuel* **1984**, *63*, 190–196.

(26) Moore, P. K.; Akgerman, A. Comments on Upgrading of Middle Distillate Fractions of a Syncrude from Athabasca Oil Sands. *Fuel* **1985**, *64*, 721–722.

(27) Yuan, T.; Marshall, W. D. Catalytic Hydrogenation of Polycyclic Aromatic Hydrocarbons over Palladium/γ-Al_2O_3 under Mild Conditions. *J. Hazard. Mater.* **2005**, *B126*, 149–157.

Received for review July 20, 2010
Revised manuscript received September 30, 2010
Accepted November 9, 2010

IE101550G